

Transfer Learning for EEG-Based Brain–Computer Interfaces: A Review of Progress Made Since 2016

Dongrui Wu^{1b}, Senior Member, IEEE, Yifan Xu, Graduate Student Member, IEEE,
and Bao-Liang Lu^{1b}, Senior Member, IEEE

Abstract—A brain–computer interface (BCI) enables a user to communicate with a computer directly using brain signals. The most common noninvasive BCI modality, electroencephalogram (EEG), is sensitive to noise/artifact and suffers between-subject/within-subject nonstationarity. Therefore, it is difficult to build a generic pattern recognition model in an EEG-based BCI system that is optimal for different subjects, during different sessions, for different devices and tasks. Usually, a calibration session is needed to collect some training data for a new subject, which is time consuming and user unfriendly. Transfer learning (TL), which utilizes data or knowledge from similar or relevant subjects/sessions/devices/tasks to facilitate learning for a new subject/session/device/task, is frequently used to reduce the amount of calibration effort. This article reviews journal publications on TL approaches in EEG-based BCIs in the last few years, i.e., since 2016. Six paradigms and applications—motor imagery, event-related potentials, steady-state visual evoked potentials, affective BCIs, regression problems, and adversarial attacks—are considered. For each paradigm/application, we group the TL approaches into cross-subject/session, cross-device, and cross-task settings and review them separately. Observations and conclusions are made at the end of the article, which may point to future research directions.

Index Terms—Adversarial attacks, affective brain–computer interface (BCI), brain–computer interfaces, domain adaptation, electroencephalogram (EEG), transfer learning (TL).

Manuscript received May 6, 2020; revised June 16, 2020; accepted July 2, 2020. Date of publication July 7, 2020; date of current version March 11, 2022. The work of Dongrui Wu and Yifan Xu was supported in part by the Hubei Province Funds for Distinguished Young Scholars under Grant 2020CFA050; in part by the Hubei Technology Innovation Platform under Grant 2019AEA171; in part by the National Natural Science Foundation of China under Grant 61873321 and Grant U1913207; and in part by the International Science and Technology Cooperation Program of China under Grant 2017YFE0128300. The work of Bao-Liang Lu was supported in part by the National Key Research and Development Program of China under Grant 2017YFB1002501; in part by the National Natural Science Foundation of China under Grant 61673266 and Grant 61976135; in part by SJTU Transmed Awards Research under Grant WF540162605; in part by the Fundamental Research Funds for the Central Universities; and in part by the 111 Project. (Corresponding author: Dongrui Wu.)

Dongrui Wu and Yifan Xu are with the Ministry of Education Key Laboratory of Image Processing and Intelligent Control, School of Artificial Intelligence and Automation, Huazhong University of Science and Technology, Wuhan 430074, China (e-mail: drwu@hust.edu.cn; yfxu@hust.edu.cn).

Bao-Liang Lu is with the Center for Brain-Like Computing and Machine Intelligence, Department of Computer Science and Engineering, Key Laboratory of Shanghai Education Commission for Intelligent Interaction and Cognitive Engineering, Brain Science and Technology Research Center, and the Qing Yuan Research Institute, Shanghai Jiao Tong University, Shanghai 200240, China (e-mail: bllu@sjtu.edu.cn).

Color versions of one or more figures in this article are available at <https://doi.org/10.1109/TCDS.2020.3007453>.

Digital Object Identifier 10.1109/TCDS.2020.3007453

I. INTRODUCTION

A BRAIN–COMPUTER interface (BCI) enables a user to communicate with a computer using his/her brain signals directly [1], [2]. The term was first coined by Vidal in 1973 [3], although it had been studied previously [4], [5]. BCIs were initially proposed for disabled people [6], but their current application scope has been extended to able-bodied users [7], in gaming [8], emotion recognition [9], mental fatigue evaluation [10], vigilance estimation [11], [12], etc.

There are generally three types of BCIs [13].

- 1) *Noninvasive BCIs*, which use noninvasive brain signals measured outside of the brain, e.g., electroencephalograms (EEGs) and functional near-infrared spectroscopy (fNIRS).
- 2) *Invasive BCIs*, which require surgery to implant sensor arrays or electrodes within the gray matter under the scalp to measure and decode brain signals (usually spikes and local field potentials).
- 3) *Partially invasive (semiinvasive) BCIs*, in which the sensors are surgically implanted inside the skull but outside the brain rather than within the gray matter.

This article focuses on noninvasive BCIs, particularly EEG-based BCIs, which are the most popular type of BCIs due to their safety, low cost, and convenience.

A closed-loop EEG-based BCI system, shown in Fig. 1, consists of the following components.

- 1) *Signal acquisition* [14], which uses an EEG device to collect EEG signals from the scalp. In the early days, EEG devices used wired connections and gel to increase conductivity. Currently, wireless connections and dry electrodes are becoming increasingly popular.
- 2) *Signal processing* [15], which usually includes temporal filtering and spatial filtering. The former typically uses a bandpass filter to reduce interference and noise, such as muscle artifacts, eye blinks, and DC drift. The latter combines different EEG channels to increase the signal-to-noise ratio. Popular spatial filters include common spatial patterns (CSPs) [16], independent component analysis (ICA) [17], blind source separation [18], xDAWN [19], etc.
- 3) *Feature extraction*, for which time domain, frequency domain [20], time–frequency domain, Riemannian space [21], and/or functional brain connectivity [22] features could be used.
- 4) *Pattern recognition*, where depending on the application, a classifier or regression model is used.

5) *Controller*, which outputs a command to control an external device, e.g., a wheelchair or a drone, or to alter the behavior of an environment, e.g., the difficulty level of a video game. A controller may not be needed in certain applications, e.g., BCI spellers.

When deep learning is used, feature extraction and pattern recognition can be integrated into a single neural network, and both components are optimized simultaneously and automatically.

EEG signals are weak, easily contaminated by interference and noise, nonstationary for the same subject, and varying across different subjects and sessions. Therefore, it is challenging to build a universal machine learning model in an EEG-based BCI system that is optimal for different subjects, during different sessions, and for different devices and tasks. Usually, a calibration session is needed to collect some training data for a new subject, which is time consuming and user unfriendly. Therefore, reducing this subject-specific calibration is critical to the market success of EEG-based BCIs.

Different machine learning techniques, e.g., transfer learning (TL) [23] and active learning [24], have been used for this purpose. Among them, TL is particularly promising because it can utilize data or knowledge from similar or relevant subjects/sessions/devices/tasks to facilitate learning for a new subject/session/device/task. Moreover, it may also be integrated with other machine learning techniques, e.g., active learning [25], [26], for even better performance. This article focuses on TL in EEG-based BCIs.

There are three classic classification paradigms in EEG-based BCIs, which will be considered in this article as follows.

- 1) Motor imagery (MI) [27], which can modify neuronal activity in primary sensorimotor areas, is similar to a real executed movement. As different MIs affect different regions of the brain, e.g., the left (right) hemisphere for right-hand (left-hand) MI and center for feet MI, a BCI can decode MI from the EEG signals and map it to a specific command.
- 2) Event-related potentials (ERPs) [28], [29], which are any stereotyped EEG responses to a visual, audio, or tactile stimulus. The most frequently used ERP is P300 [30], which occurs approximately 300 ms after a rare stimulus.
- 3) Steady-state visual evoked potentials (SSVEPs) [31], in which EEG oscillates at the same (or multiples of) frequency of the visual stimulus at a specific frequency, usually between 3.5 and 75 Hz [32]. This paradigm is frequently used in BCI spellers [33], as it can achieve a very high information transfer rate.

EEG-based affective BCIs (aBCIs) [34]–[37], which detect affective states (moods, emotions) from EEGs and use them in BCIs, have become an emerging research area. There are also some interesting regression problems in EEG-based BCIs, e.g., driver drowsiness estimation [38]–[40] and user reaction time estimation [41]. Additionally, a recent research [42], [43] has shown that BCIs also suffer from adversarial attacks, where deliberately designed tiny perturbations are added to benign EEG trials to fool the machine learning model and cause

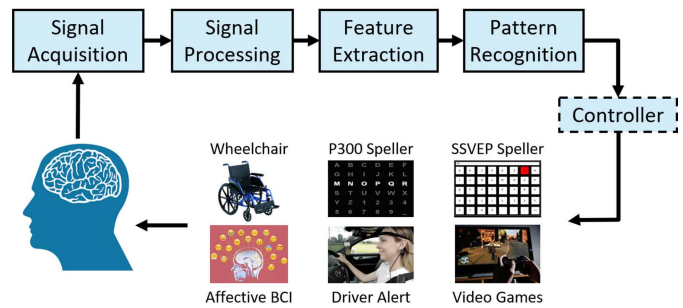


Fig. 1. Flowchart of a closed-loop EEG-based BCI system.

dramatic performance degradation. This article also considers aBCIs, regression problems, and adversarial attacks of EEG-based BCIs.

Although TL has been applied in all of the above EEG-based BCI paradigms and applications, to the best of our knowledge, there is no comprehensive and up-to-date review on it. Wang *et al.* [44] performed a short review in a conference paper in 2015. Jayaram *et al.* [45] gave a brief review in 2016, considering only cross-subject and cross-session transfers. Lotte *et al.* [46] provided a comprehensive review of classification algorithms for EEG-based BCIs between 2007 and 2017. Again, they only considered cross-subject and cross-session transfers. Azab *et al.* [47] performed a review of four categories of TL approaches in BCIs in 2018: 1) instance-based TL; 2) feature-representation TL; 3) classifier-based TL; and 4) relational-based TL.

However, all the aforementioned reviews considered only cross-subject and cross-session TL of the three classic paradigms of EEG-based BCIs (MI, ERP, and SSVEP) but did not mention the more challenging cross-device and cross-task transfers, aBCIs, regression problems, and adversarial attacks.

To fill these gaps and to avoid overlapping too much with previous reviews, this article reviews journal publications of TL approaches in EEG-based BCIs in the last few years, i.e., since 2016. Six paradigms and applications are considered: 1) MI; 2) ERP; 3) SSVEP; 4) aBCI; 5) regression problems; and 6) adversarial attacks. For each paradigm/application, we group the TL approaches into cross-subject/session (because these two concepts are essentially the same), cross-device, and cross-task settings and review them separately, unless no TL approaches have been proposed for that category. Some TL approaches may cover more than two categories, e.g., both cross-subject and cross-device transfers were considered. In this case, we introduce them in the more challenging category, e.g., cross-device TL. When there are multiple TL approaches in each category, we generally introduce them according to the years in which they were proposed, unless there are intrinsic connections among several approaches.

The remainder of this article is organized as follows. Section II briefly introduces some basic concepts of TL. Sections III–VIII review TL approaches in MI, ERP, SSVEP, aBCIs, regression problems, and adversarial attacks, respectively. Section IX makes observations and conclusions, which may point to some future research directions.

II. TL CONCEPTS AND SCENARIOS

This section introduces the basic definitions of TL, some related concepts, e.g., domain adaptation and covariate shift, and different TL scenarios in EEG-based BCIs.

In machine learning, a feature vector is usually denoted by a bold symbol \mathbf{x} . To emphasize that each EEG trial is a 2-D matrix, this article denotes a trial by $X \in \mathbb{R}^{E \times T}$, where E is the number of electrodes and T is the number of time-domain samples. Of course, X can also be converted into a feature vector \mathbf{x} .

A. TL Concepts

Definition 1: A domain [23], [48] \mathcal{D} consists of a feature space \mathcal{X} and its associated marginal probability distribution $P(X)$, i.e., $\mathcal{D} = \{\mathcal{X}, P(X)\}$, where $X \in \mathcal{X}$.

A source domain \mathcal{D}_s and a target domain \mathcal{D}_t are different if they have different feature spaces, i.e., $\mathcal{X}_s \neq \mathcal{X}_t$, and/or different marginal probability distributions, i.e., $P_s(X) \neq P_t(X)$.

Definition 2: Given a domain \mathcal{D} , a task [23], [48] \mathcal{T} consists of a label space \mathcal{Y} and a prediction function $f(X)$, i.e., $\mathcal{T} = \{\mathcal{Y}, f(X)\}$.

Let $y \in \mathcal{Y}$. Then, $f(X) = P(y|X)$ is the conditional probability distribution. Two tasks \mathcal{T}_s and \mathcal{T}_t are different if they have different label spaces, i.e., $\mathcal{Y}_s \neq \mathcal{Y}_t$, and/or different conditional probability distributions, i.e., $P_s(y|X) \neq P_t(y|X)$.

Definition 3: Given a source domain $\mathcal{D}_s = \{(X_s^i, y_s^i)\}_{i=1}^{N_s}$ and a target domain \mathcal{D}_t with N_t labeled samples $\{(X_t^i, y_t^i)\}_{i=1}^{N_t}$ and N_u unlabeled samples $\{X_t^i\}_{i=N_t+1}^{N_t+N_u}$, TL aims to learn a target prediction function $f : X_t \mapsto y_t$ with low expected error on \mathcal{D}_t under the general assumptions that $\mathcal{X}_s \neq \mathcal{X}_t$, $\mathcal{Y}_s \neq \mathcal{Y}_t$, $P_s(X) \neq P_t(X)$, and/or $P_s(y|X) \neq P_t(y|X)$.

In *inductive TL*, the target domain has some labeled samples, i.e., $N_t > 0$. For most inductive TL scenarios in BCIs, the source domain samples are labeled, but they could also be unlabeled. When the source domain samples are labeled, inductive TL is similar to *multitask learning* [49]. The difference is that multitask learning tries to learn a model for every domain simultaneously, whereas inductive TL focuses only on the target domain. In *transductive TL*, the source domain samples are all labeled, but the target domain samples are all unlabeled, i.e., $N_t = 0$. In *unsupervised TL*, no samples in either domain are labeled.

Domain adaptation is a special case of TL, or more specifically, transductive TL.

Definition 4: Given a source domain \mathcal{D}_s and a target domain \mathcal{D}_t , *domain adaptation* aims to learn a target prediction function $f : \mathbf{x}_t \mapsto y_t$ with low expected error on \mathcal{D}_t , under the assumptions that $\mathcal{X}_s = \mathcal{X}_t$ and $\mathcal{Y}_s = \mathcal{Y}_t$, but $P_s(X) \neq P_t(X)$ and/or $P_s(y|X) \neq P_t(y|X)$.

Covariate shift is a special and simpler case of domain adaptation.

Definition 5: Given a source domain \mathcal{D}_s and a target domain \mathcal{D}_t , *covariate shift* occurs when $\mathcal{X}_s = \mathcal{X}_t$, $\mathcal{Y}_s = \mathcal{Y}_t$, $P_s(y|X) = P_t(y|X)$, but $P_s(X) \neq P_t(X)$.

B. TL Scenarios

According to the variations between the source and the target domains, there can be different TL scenarios in EEG-based BCIs.

- 1) *Cross-Subject TL:* Data from other subjects (the source domains) are used to facilitate the calibration for a new subject (the target domain). Usually, the task and EEG device are the same across subjects.
- 2) *Cross-Session TL:* Data from previous sessions (the source domains) are used to facilitate the calibration of a new session (the target domain). For example, data from previous days are used in the current calibration. Usually, the subject, task, and EEG device are the same across sessions.
- 3) *Cross-Device TL:* Data from one EEG device (the source domain) are used to facilitate the calibration of a new device (the target domain). Usually, the task and subject are the same across EEG devices.
- 4) *Cross-Task TL:* Labeled data from other similar or relevant tasks (the source domains) are used to facilitate the calibration for a new task (the target domain). For example, data from left- and right-hand MI are used in the calibration of feet and tongue MI. Usually, the subject and EEG device are the same across tasks.

Since cross-subject TL and cross-session TL are essentially the same, this article combines them into one category: cross-subject/session TL. Generally, cross-device TL and cross-task TL are more challenging than cross-subject/session TL; hence, they were less studied in the literature.

The above simple TL scenarios could also be mixed to form more complex TL scenarios, e.g., cross-subject and cross-device TL [26], cross-subject and cross-task TL [50], etc.

III. TL IN MI-BASED BCIS

This section reviews recent progress in TL for MI-based BCIs. Many of them used the BCI competition data sets.¹

Assume there are S source domains, and the s th source domain has N_s EEG trials. The n th trial of the s th source domain is denoted by $X_s^n \in \mathbb{R}^{E \times T}$, where E is the number of electrodes and T is the number of time-domain samples from each channel. The corresponding covariance matrix is $C_s^n \in \mathbb{R}^{E \times E}$, which is symmetric and positive definite (SPD) and lies on a Riemannian manifold. For binary classification, the label for X_s^n is $y_s^n \in \{-1, 1\}$. The n th EEG trial in the target domain is denoted by X_t^n , and the covariance matrix is denoted by C_t^n . These notations are used throughout this article.

A. Cross-Subject/Session Transfer

Dai *et al.* [51] proposed the transfer kernel CSPs (TKCSPs) method, which integrates kernel CSPs (KCSPs) [52] and transfer kernel learning (TKL) [53] for EEG trial spatial filtering in cross-subject MI classification. It first computes a domain-invariant kernel by TKL and then uses it in the KCSP approach, which further finds the components with the largest

¹<http://www.bbc.de/competition/>

energy difference between two classes. Note that TL was used in EEG signal processing (spatial filtering) instead of classification.

Jayaram *et al.* [45] proposed a multitask learning framework for cross-subject/session transfers, which does not need any labeled data in the target domain. The linear decision rule is $y = \text{sign}(\boldsymbol{\mu}_\alpha^T X \boldsymbol{\mu}_w)$, where $\boldsymbol{\mu}_\alpha \in \mathbb{R}^{C \times 1}$ are the channel weights and $\boldsymbol{\mu}_w \in \mathbb{R}^{T \times 1}$ are the feature weights. $\boldsymbol{\mu}_\alpha$ and $\boldsymbol{\mu}_w$ are obtained by minimizing

$$\min_{\boldsymbol{\alpha}_s, \boldsymbol{w}_s} \left[\frac{1}{\lambda} \sum_{s=1}^S \sum_{n=1}^{N_s} \|\boldsymbol{\alpha}_s^T X_s^n \boldsymbol{w}_s - y_s^n\|^2 + \sum_{s=1}^S \Omega(\boldsymbol{w}_s; \boldsymbol{\mu}_w, \boldsymbol{\Sigma}_w) + \sum_{s=1}^S \Omega(\boldsymbol{\alpha}_s; \boldsymbol{\mu}_\alpha, \boldsymbol{\Sigma}_\alpha) \right] \quad (1)$$

where $\boldsymbol{\alpha}_s \in \mathbb{R}^{C \times 1}$ are the channel weights for the s th source subject, $\boldsymbol{w}_s \in \mathbb{R}^{T \times 1}$ are the feature weights, λ is a hyperparameter, and $\Omega(\boldsymbol{w}_s; \boldsymbol{\mu}_w, \boldsymbol{\Sigma}_w)$ is the negative log prior probability of \boldsymbol{w}_s given the Gaussian distribution parameterized by $(\boldsymbol{\mu}_w, \boldsymbol{\Sigma}_w)$. $\boldsymbol{\mu}_w$ and $\boldsymbol{\Sigma}_w$ ($\boldsymbol{\mu}_\alpha$ and $\boldsymbol{\Sigma}_\alpha$) is the mean vector and covariance matrix of $\{\boldsymbol{w}_s\}_{s=1}^S$ ($\{\boldsymbol{\alpha}_s\}_{s=1}^S$), respectively.

In (1), the first term requires $\boldsymbol{\alpha}_s$ and \boldsymbol{w}_s to work well for the s th source subject; the second term ensures that the divergence of \boldsymbol{w}_s from the shared $(\boldsymbol{\mu}_w, \boldsymbol{\Sigma}_w)$ is small, i.e., all the source subjects should have similar \boldsymbol{w}_s values; and the third term ensures that the divergence of $\boldsymbol{\alpha}_s$ from the shared $(\boldsymbol{\mu}_\alpha, \boldsymbol{\Sigma}_\alpha)$ is small. $\boldsymbol{\mu}_\alpha$ and $\boldsymbol{\mu}_w$ can be viewed as the subject-invariant characteristics of stimulus prediction, and hence used directly by a new subject. Jayaram *et al.* demonstrated that their approach worked well on cross-subject transfers in MI classification and cross-session transfers for one patient with amyotrophic lateral sclerosis.

Azab *et al.* [54] proposed weighted TL for cross-subject transfers in MI classification as an improvement of the above approach. They assumed that each source subject has plenty of labeled samples, whereas the target subject has only a few labeled samples. They first trained a logistic regression classifier for each source subject by using a cross-entropy loss function with an L2 regularization term. Then, a logistic regression classifier for the target subject was trained so that the cross-entropy loss of the few labeled samples in the target domain is minimized, and its parameters are close to those of the source subjects. The mean vector and covariance matrix of the classifier parameters in the source domains were computed in a similar way to that in [45], except that for each source domain, a weight determined by the Kullback–Leibler divergence between it and the target domain was used.

Hossain *et al.* [55] proposed an ensemble learning approach for cross-subject transfers in multiclass MI classification. Four base classifiers were used, all constructed using TL and active learning: 1) multiclass direct transfer with active learning (mDTAL), a multiclass extension of the active TL approach proposed in [56]; 2) multiclass aligned instance transfer with active learning, which is similar to mDTAL except that only the source-domain samples correctly classified by the corresponding classifier are transferred; 3) most informative and

aligned instances transfer with active learning, which transfers only the source-domain samples correctly classified by its classifiers and near the decision boundary (i.e., the most informative samples); and 4) most informative instances transfer with active learning, which transfers only source-domain samples close to the decision boundary. The four base learners were finally stacked to achieve more robust performance.

Since the covariance matrices of EEG trials are SPD and lie on a Riemannian manifold instead of in the Euclidean space, Riemannian approaches [21] have become popular in EEG-based BCIs. Different TL approaches have also been proposed recently.

Zanini *et al.* [57] proposed a Riemannian alignment (RA) approach to centre the EEG covariance matrices $\{C_k^n\}_{n=1}^{N_k}$ in the k th domain with respect to a reference covariance matrix \bar{R}_k specific to that domain. More specifically, RA computes first the covariance matrices of some *resting* trials in the k th domain, in which the subject is not performing any task, and then calculates their Riemannian mean \bar{R}_k . \bar{R}_k is next used as the reference matrix to reduce the intersubject/session variation

$$\tilde{C}_k^n = \bar{R}_k^{-\frac{1}{2}} C_k^n \bar{R}_k^{-\frac{1}{2}} \quad (2)$$

where \tilde{C}_k^n is the aligned covariance matrix for C_k^n . Equation (2) centers the reference state of different subjects/sessions at the identity matrix. In MI, the resting state is the time window during which the subject is not performing any task, e.g., the transition window between two MI tasks. In ERP, the nontarget stimuli are used as the resting state, requiring that some labeled trials in the target domain must be known. Zanini *et al.* also proposed improvements to the minimum distance to the Riemannian mean (MDRM) [58] classifier and demonstrated the effectiveness of RA and the improved MDRM in both MI and ERP classifications.

Yair *et al.* [59] proposed a domain adaptation approach using the analytic expression of parallel transport (PT) on the cone manifold of SPD matrices. The goal was to find a common tangent space such that the mappings of C_l and C_s are aligned. It first computes the Riemannian mean \bar{R}_k of the k th domain and then the Riemannian mean \hat{R} of all \bar{R}_k . Then, each \bar{R}_k is moved to \hat{R} by PT $\Gamma_{\bar{R}_k \rightarrow \hat{R}}$, and C_k^n , the n th covariance matrix in the k th domain, is projected to

$$\text{Log}\left(\hat{R}^{-\frac{1}{2}} \Gamma_{\bar{R}_k \rightarrow \hat{R}}(C_k^n) \hat{R}^{-\frac{1}{2}}\right) = \text{Log}\left(\bar{R}_k^{-\frac{1}{2}} C_k^n \bar{R}_k^{-\frac{1}{2}}\right). \quad (3)$$

After the projection step, the covariance matrices in different domains are mapped to the same tangent space, so a classifier built in a source domain can be directly applied to the target domain. Equation (3) is essentially identical to RA in (2), except that (3) works in the tangent space, whereas (2) works in the Riemannian space. Yair *et al.* demonstrated the effectiveness of PT in cross-subject MI classification, sleep stage classification, and mental arithmetic identification.

To make RA more flexible, faster, and completely unsupervised, He and Wu [60] proposed a Euclidean alignment (EA) approach to align EEG trials from different subjects in the Euclidean space. Mathematically, for the k th domain, EA computes the reference matrix $\bar{R}_k = (1/N) \sum_{n=1}^N X_k^n (X_k^n)^T$, i.e., \bar{R}_k is the arithmetic mean of all covariance matrices in

the k th domain (it can also be the Riemannian mean, which is more computationally intensive than the arithmetic mean), then performs the alignment by $\tilde{X}_k^n = \bar{R}_k^{-(1/2)} X_k^n$. After EA, the mean covariance matrices of all domains become the identity matrix. Both Euclidean space and Riemannian space feature extraction and classification approaches can then be applied to \tilde{X}_k^n . EA can be viewed as a generalization of Yair *et al.*'s PT approach because the computation of \bar{R}_k in EA is more flexible, and both Euclidean and Riemannian space classifiers can be used after EA. He and Wu demonstrated that EA outperformed RA in both MI and ERP classifications in both offline and simulated online applications.

Rodrigues *et al.* [61] proposed the Riemannian procrustes analysis (RPA) to accommodate covariant shifts in EEG-based BCIs. It is semisupervised and requires at least one labeled sample from each target-domain class. RPA first matches the statistical distributions of the covariance matrices of the EEG trials from different domains, using simple geometrical transformations, namely, translation, scaling, and rotation, in sequence. Then, the labeled and transformed data from both domains are concatenated to train a classifier, which is next applied to the transformed and unlabeled target domain samples. Mathematically, it transforms each target domain covariance matrix C_t^n into

$$\tilde{C}_t^n = M_s^{\frac{1}{2}} \left[U^T \left(\tilde{M}_t^{-\frac{1}{2}} C_t^n \tilde{M}_t^{-\frac{1}{2}} \right)^p U \right] M_s^{\frac{1}{2}} \quad (4)$$

where

$\tilde{M}_t^{-(1/2)}$ is the geometric mean of the labeled target domain samples, which centers the target-domain covariance matrices at the identity matrix;

$p = (d/\tilde{d})^{(1/2)}$ stretches the target-domain covariance matrices so that they have the same dispersion as the source domain, in which d and \tilde{d} are the dispersions around the geometric mean of the source domain and the target domain, respectively;

U is an orthogonal rotation matrix to be optimized, which minimizes the distance between the class means of the source domain and the translated and stretched target domain;

$M_s^{-(1/2)}$ is the geometric mean of the labeled source domain samples, which ensures that the geometric mean of \tilde{C}_t^n is the same as that in the source domain.

Note that the class label information is only needed in computing U . Although $\tilde{M}_t^{-(1/2)}$, p , and $M_s^{-(1/2)}$ are also computed from the labeled samples, they do not need the specific class labels.

Clearly, RPA is a generalization of RA. Rodrigues *et al.* [61] showed that RPA can achieve promising results in cross-subject MI, ERP, and SSVEP classification.

Recently, Zhang and Wu [62] proposed a manifold embedded knowledge transfer (MEKT) approach, which first aligns the covariance matrices of the EEG trials in the Riemannian manifold, extracts features in the tangent space, and then performs domain adaptation by minimizing the joint probability

distribution shift between the source and the target domains while preserving their geometric structures. More specifically, it consists of the following three steps [62].

- 1) *Covariance Matrix Centroid Alignment (CA)*: Align the centroid of the covariance matrices in each domain, i.e., $\tilde{C}_s^n = \bar{R}_s^{-(1/2)} C_s^n \bar{R}_s^{-(1/2)}$ and $\tilde{C}_t^n = \bar{R}_t^{-(1/2)} C_t^n \bar{R}_t^{-(1/2)}$, where \bar{R}_s (\bar{R}_t) can be the Riemannian mean, the Euclidean mean, or the log-Euclidean mean of all C_s^n (C_t^n). This is essentially a generalization of RA [57]. The marginal probability distributions from different domains are brought together after CA.
- 2) *Tangent Space Feature Extraction*: Map and assemble all \tilde{C}_s^n (\tilde{C}_t^n) into a tangent space super matrix $\tilde{X}_s \in \mathbb{R}^{d \times N_s}$ ($\tilde{X}_t \in \mathbb{R}^{d \times N_t}$), where $d = E(E+1)/2$ is the dimensionality of the tangent space features.
- 3) *Mapping Matrices Identification*: Find the projection matrices $A \in \mathbb{R}^{d \times p}$ and $B \in \mathbb{R}^{d \times p}$, where $p \ll d$ is the dimensionality of the shared subspace such that $A^T \tilde{X}_s$ and $B^T \tilde{X}_t$ are similar.

After MEKT, a classifier can be trained on $(A^T \tilde{X}_s, y_s)$ and applied to $B^T \tilde{X}_t$ to estimate their labels.

MEKT can cope with one or more source domains and still be efficient. Zhang and Wu [62] also used domain transferability estimation (DTE) to identify the most beneficial source domains, in case there are too many of them. Experiments in cross-subject MI and ERP classification demonstrated that MEKT outperformed several state-of-the-art TL approaches, and DTE can reduce the computational cost to more than half of when the number of source domains is large, with little sacrifice of classification accuracy.

A comparison of the aforementioned EEG data alignment approaches, and a new approach [50] introduced later in this section, is given in Table I.

Singh *et al.* [63] proposed a TL approach for estimating the sample covariance matrices, which are used by the MDRM classifier, from a very small number of target-domain samples. It first estimates the sample covariance matrix for each class by a weighted average of the sample covariance matrix of the corresponding class from the target domain and that in the source domain. The mixed sample covariance matrix is the sum of the per-class sample covariance matrices. Spatial filters are then computed from the mixed and per-class sample covariance matrices. Next, the covariance matrices of the spatially filtered EEG trials are further filtered by a Fisher geodesic discriminant analysis [64] and used as features in the MDRM [58] classifier.

Deep learning, which has been very successful in image processing, video analysis, speech recognition, and natural language processing, has also started to find applications in EEG-based BCIs. For example, Schirmer *et al.* [65] proposed two convolutional neural networks (CNNs) for EEG decoding and showed that both outperformed filter bank CSPs (FBCSPs) [66] in cross-subject MI classification. Lawhern *et al.* [67] proposed EEGNet, a compact CNN architecture for EEG classification. It can be applied across different BCI paradigms, be trained with very limited data, and generate neurophysiologically interpretable features. EEGNet achieved robust results in both the within-subject and cross-subject classification of MIs and ERPs.

TABLE I
COMPARISON OF DIFFERENT EEG DATA ALIGNMENT APPROACHES

	RA [57]	PT [59]	PTA [61]	EA [60]	CA [62]	LA [50]
Applicable Paradigm	MI, ERP	MI	MI, ERP, SSVEP	MI, ERP	MI, ERP	MI
Online or Offline	Both	Both	Both	Both	Both	Offline
Need Labeled Target Domain Trials	No for MI, Yes for ERP	No	Yes	No	No	Yes
What to Align	Riemannian space covariance matrices	Riemannian Tangent space features	Riemannian space covariance matrices	Euclidean space EEG trials	Riemannian space covariance matrices	Euclidean space EEG trials
Reference Matrix Calculation	Riemannian mean of resting state covariance matrices in each domain	Riemannian mean of all covariance matrices in each domain	Riemannian mean of all labeled covariance matrices in each domain	Euclidean mean of all covariance matrices in each domain	Riemannian, Euclidean, or Log-Euclidean mean of all covariance matrices in each domain	Log-Euclidean mean of labeled covariance matrices in each class of each domain
Classifier	Riemannian space only	Euclidean space only	Riemannian space only	Riemannian or Euclidean space	Riemannian or Euclidean space	Riemannian or Euclidean space
Handle Class Mismatch between Domains	No	No	No	No	No	Yes
Computational Cost	High	High	High	Low	Low	Low

Although the above approaches achieved promising cross-subject classification performance, they did not explicitly use the idea of TL. Currently, a common TL technique for deep learning-based EEG classification [68], [69] is based on fine tuning with new data from the target session/subject. Unlike concatenating target data with the existing source data, the fine-tuning process is established on a pretrained model and performs iterative learning on a relatively small amount of target data. Although the training data involved are exactly the same as using data concatenation, the prediction performance can be improved significantly.

More specifically, Wu *et al.* [70] proposed a parallel multiscale filter CNN for MI classification. It consisted of three layers: 1) a CNN to extract both temporal and spatial features from EEG signals; 2) a feature reduction layer with square and log nonlinear functions followed by pooling and dropout; and 3) a dense classification layer fine tuned on a small amount of calibration data from the target subject. They showed that fine tuning achieved improved performance in cross-subject transfers.

B. Cross-Device TL

Xu *et al.* [71] studied the performance of deep learning in cross-data set TL. Eight publicly available MI data sets were considered. Although the different data sets used different EEG devices, channels, and MI tasks, they only selected three common channels (C3, CZ, and C4) and the left-hand and right-hand MI tasks. They applied an online prealignment strategy to each EEG trial of each subject by recursively computing the Riemannian mean online and using it as the reference matrix in the EA approach. They showed that online prealignment significantly increased the performance of deep learning models in cross-data set TL.

C. Cross-Task TL

Both RA and EA assume that the source domains have the same feature space and label space as the target domain, which

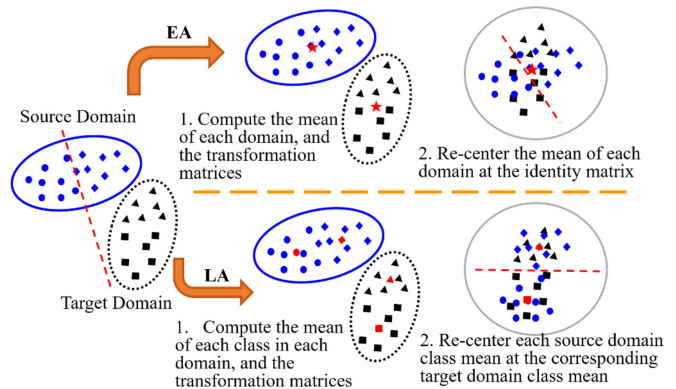


Fig. 2. Illustration of EA and LA [50].

may not hold in many real-world applications, i.e., they may not be used in cross-task transfers. Recently, He and Wu [50] also proposed a label alignment (LA) approach, which can handle the situation that the source domains have different label spaces from the target domain. For MI-based BCIs, this means the source subjects and the target subject can perform completely different MI tasks (e.g., the source subject may perform left-hand and right-hand MI tasks, whereas the target subject may perform feet and tongue MIs), but the source subjects' data can still be used to facilitate the calibration for a target subject.

When the source- and target-domain devices are different, LA first selects the source EEG channels that are the most similar to the target EEG channels. Then, it computes the mean covariance matrix of each source-domain class and estimates the mean covariance matrix of each target-domain class. Next, it recenters each source-domain class at the corresponding estimated class mean of the target domain. Both Euclidean space and Riemannian space feature extraction and classification approaches can next be applied to aligned trials. LA

only needs as few as one labeled sample from each target-domain class, can be used as a preprocessing step before different feature extraction and classification algorithms, and can be integrated with other TL approaches to achieve even better performance. He and Wu [50] demonstrated the effectiveness of LA in simultaneous cross-subject, cross-device, and cross-task TL in MI classification.

An illustration of the difference between LA and EA is shown in Fig. 2. To the best of our knowledge, LA is the only cross-task TL work in EEG-based BCIs and the most complicated TL scenario (simultaneous cross-subject, cross-device, and cross-task TL) considered in the literature so far.

IV. TL IN ERP-BASED BCIS

This section reviews recent TL approaches in ERP-based BCIs. Many approaches introduced in the previous section, e.g., RA, EA, RPA, and EEGNet, can also be used here. To avoid duplication, we only include approaches not introduced in the previous section here. Because there were no publications on cross-task TL in ERP-based BCIs, we do not have a “cross-task TL” section.

A. Cross-Subject/Session TL

Waytowich *et al.* [72] proposed unsupervised spectral transfer method using information geometry (STIG) for subject-independent ERP-based BCIs. STIG uses a spectral metalearner [73] to combine predictions from an ensemble of MDRM classifiers on data from individual source subjects. Experiments on single-trial ERP classification demonstrated that STIG significantly outperformed some calibration-free approaches and traditional within-subject calibration approaches when limited data were available in both offline and online ERP classifications.

Wu [74] proposed weighted adaptation regularization (wAR) for cross-subject transfers in ERP-based BCIs in both online and offline settings. Mathematically, wAR learns the following classifier directly:

$$\begin{aligned} \operatorname{argmin}_f & \sum_{n=1}^{N_s} w_s^n \ell(f(X_s^n), y_s^n) + w_t \sum_{n=1}^{N_t} w_t^n \ell(f(X_t^n), y_t^n) \\ & + \sigma \|f\|_K^2 + \lambda_P D_{f,K}(P_S(X_S), P_T(X_T)) \\ & + \lambda_Q D_{f,K}(P_S(X_S|y_S), P_T(X_T|y_T)) \end{aligned} \quad (5)$$

where ℓ is a loss function, w_t is the overall weight of target domain samples, K is a kernel function, and σ , λ_P , and λ_Q are nonnegative regularization parameters. w_s^n and w_t^n are the weights for the n th sample in the source domain and the target domain, respectively, to balance the number of positive and negative samples in the corresponding domain.

Briefly, the five terms in (5) minimize the fitting loss in the source domain, the fitting loss in the target domain, the structural risk of the classifier, the distance between the marginal probability distributions $P_S(X_S)$ and $P_T(X_T)$, and the distance between the conditional probability distributions $P_S(X_S|y_S)$ and $P_T(X_T|y_T)$. Experiments on single-trial visual evoked potential classification demonstrated that both online and offline wAR algorithms were effective. Wu [74] also proposed a

source-domain selection approach, which selects the most beneficial source subjects for transferring. It can reduce the computational cost of wAR by $\sim 50\%$ without sacrificing the classification performance.

Qi *et al.* [75] performed cross-subject TL on a P300 speller to reduce the calibration time. A small set of ERP epochs from the target subject was used as a reference to compute the Riemannian distance to each source ERP sample from an existing data pool. The most similar ones were selected to train a classifier and were applied to the target subject.

Jin *et al.* [76] used a generic model set to reduce the calibration time in P300-based BCIs. Filtered EEG data from 116 participants were assembled into a data matrix, the principal component analysis (PCA) was used to reduce the dimensionality of the time domain features, and then 116 participants were clustered into ten groups by k -means clustering. A weighted linear discriminant analysis (WLDA) classifier was then trained for each cluster. These ten classifiers formed the generic model set. For a new subject, a few calibration samples were acquired and an online linear discriminant (OLDA) model was trained. The OLDA model was matched to the closest WLDA model, which was then selected as the model for the new subject.

Deep learning has also been used in ERP classification. Inspired by generative adversarial networks (GANs) [77], Ming *et al.* [78] proposed a subject adaptation network (SAN) to mitigate individual differences in EEGs. Based on the characteristics of the application, they designed an artificial low-dimensional distribution and forced the transformed EEG features to approximate it. For example, for two-class visual evoked potential classification, the artificial distribution is bimodal, and the area of each modal is proportional to the number of samples in the corresponding class. Experiments on cross-subject visual evoked potential classification demonstrated that SAN outperformed a support vector machine (SVM) and EEGNet.

B. Cross-Device TL

Wu *et al.* [26] proposed active wAR (AwAR) for cross-device TL. It integrates wAR (introduced in Section IV-A), which uses labeled data from the previous device and handles class imbalance, and active learning [24], which selects the most informative samples from the new device to a label. Only the common channels were used in wAR, but all the channels of the new device can be used in active learning to achieve better performance. Experiments on single-trial visual evoked potential classification using three different EEG devices with different numbers of electrodes showed that AwAR can significantly reduce the calibration data requirement for a new device in offline calibration.

To the best of our knowledge, this is the only study on cross-device TL in ERP-based BCIs.

V. TL IN SSVEP-BASED BCIS

This section reviews recent TL approaches in SSVEP-based BCIs. Because there were no publications on cross-task TL in

SSVEP-based BCIs, we do not have a “cross-task TL” section. Overall, many fewer TL studies on SSVEPs have been performed compared with MI tasks and ERPs.

A. Cross-Subject/Session TL

Waytowich *et al.* [79] proposed compact-CNN, which is essentially the EEGNet [67] approach introduced in Section III-A, for 12-class SSVEP classification without the need for any user-specific calibration. It outperformed state-of-the-art hand-crafted approaches using canonical correlation analysis (CCA) and combined-CCA.

Rodrigues *et al.* [61] proposed RPA, which can also be used in cross-subject transfer of SSVEP-based BCIs. Since it has been introduced in Section III-A, it is not repeated here.

B. Cross-Device TL

Nakanishi *et al.* [80] proposed a cross-device TL algorithm for reducing the calibration effort in an SSVEP-based BCI speller. It first computes a set of spatial filters by channel averaging, CCA, or task-related component analysis and then concatenates them to form a filter matrix W . The average trial of class c of the source domain is computed and filtered by W to obtain Z_c . Let X_t be a single trial to be classified in the target domain. Its spatial filter matrix W_c is then computed by

$$W_c = \operatorname{argmin}_W \|Z_c - W^T X_t\|_2^2 \quad (6)$$

i.e., $W_c = (X_t X_t^T)^{-1} X_t Z_c^T$. Then, Pearson’s correlation coefficients between $W_c^T X_t$ and Z_c are computed as $r_c^{(1)}$, and canonical correlation coefficients between X_t and computer-generated SSVEP models Y_c are computed as $r_c^{(2)}$. The two feature values are combined as

$$\rho_c = \sum_{i=1}^2 \operatorname{sign}(r_c^{(i)}) \cdot (r_c^{(i)})^2 \quad (7)$$

and the target class is identified as $\operatorname{argmax}_c \rho_c$.

To the best of our knowledge, this is the only study on cross-device TL in SSVEP-based BCIs.

VI. TL IN ABCIS

Recently, there has been a fast-growing research interest in aBCIs [34]–[37]. Emotions can be represented by discrete categories [81] (e.g., happy, sad, and angry) and by continuous values in the 2-D space of arousal and valence [82] or the 3-D space of arousal, valence, and dominance [83]. Therefore, there can be both classification and regression problems in aBCIs. However, the current literature focused exclusively on classification problems.

Most studies used the publicly available DEAP [84] and SEED [9] data sets. DEAP consists of 32-channel EEGs recorded by a BioSemi ActiveTwo device from 32 subjects while they were watching minute-long music videos, whereas SEED consists of 62-channel EEGs recorded by an ESI NeuroScan device from 15 subjects while they were watching 4-min movie clips. By using SEED, Zheng *et al.* [85] investigated whether stable EEG patterns exist over time for emotion

recognition. Using differential entropy features, they found that stable patterns did exhibit consistency across sessions and subjects. Thus, it is possible to perform TL in aBCIs.

This section reviews the latest progress on TL in aBCIs. Because there were no publications on cross-task TL in aBCIs, we do not have a “cross-task TL” section.

A. Cross-Subject/Session TL

Chai *et al.* [86] proposed adaptive subspace feature matching (ASFm) for cross-subject and cross-session transfer in offline and simulated online EEG-based emotion classification. Differential entropy features were used. ASFm first performs PCA of the source domain and the target domain separately. Let Z_s (Z_t) be the d leading principal components in the source (target) domain, which form the corresponding subspace. Then, ASFm transforms the source-domain subspace to $Z_s Z_s^T Z_t$ and projects the source data into it. The target data are projected directly into Z_t . In this way, the marginal distribution discrepancy between the two domains is reduced. Next, an iterative pseudolabel refinement strategy is used to train a logistic regression classifier using the labeled source-domain samples and pseudolabeled target-domain samples, which can be directly applied to unlabeled target-domain samples.

Lin and Jung [87] proposed a conditional TL (cTL) framework to facilitate positive cross-subject transfers in aBCIs. Five differential laterality features (topoplots), corresponding to five different frequency bands, from each EEG channel are extracted. The cTL method first computes the classification accuracy by using the target subject’s data only and performs transfer only if that accuracy is below the chance level. Then, it uses ReliefF [88] to select a few of the most emotion-relevant features in the target domain and calculates their correlations with the corresponding features in each source domain to select a few of the most similar (correlated) source subjects. Next, the target-domain data and the selected source-domain data are concatenated to train a classifier.

Lin *et al.* [89] proposed a robust PCA (RPCA)-based [90] signal filtering strategy and validated its performance in cross-day binary emotion classification. RPCA decomposes an input matrix into the sum of a low-rank matrix and a sparse matrix. The former accounts for the relatively regular profiles of the input signals, whereas the latter accounts for its deviant events. Lin *et al.* showed that the RPCA-decomposed sparse signals filtered from the background EEG activity contributed more to the interday variability and that the predominately captured EEG oscillations of emotional responses behaved relatively consistently across days.

Li *et al.* [91] extracted nine types of time–frequency-domain features (the peak-to-peak mean, mean square, variance, Hjorth activity, Hjorth mobility, Hjorth complexity, maximum power spectral frequency, maximum power spectral density, and power sum) and nine types of nonlinear dynamical system features (the approximate entropy, C0 complexity, correlation dimension, Kolmogorov entropy, Lyapunov exponent, permutation entropy, singular entropy, Shannon entropy, and spectral entropy) from EEG measurements. Through automatic and manual feature selection, they verified the effectiveness and

performance of the upper bounds of those features in cross-subject emotion classification on DEAP and SEED. They found that L1-norm penalty-based feature selection achieved robust performance on both data sets, and the Hjorth mobility in the beta rhythm achieved the highest mean classification accuracy.

Liu *et al.* [92] performed cross-day EEG-based emotion classification. Seventeen subjects watched six to nine emotional movie clips on five different days over one month. Spectral powers of the delta, theta, alpha, beta, and low and high gamma bands were computed for each of the 60 channels as initial features, and then recursive feature elimination was used for feature selection. In cross-day classification, the data from a subset of the five days were used by an SVM to classify the data from the remaining days. They showed that EEG variability could impair the emotion classification performance dramatically, and using data from more days during training could significantly improve generalization performance.

Yang *et al.* [93] studied cross-subject emotion classification on DEAP and SEED. Ten linear and nonlinear features [the Hjorth activity, Hjorth mobility, Hjorth complexity, standard deviation, power spectral density (PSD) alpha, PSD beta, PSD gamma, PSD theta, sample entropy, and wavelet entropy] were extracted from each channel and concatenated. Then, sequential backward feature selection and significance tests were used for feature selection, and an RBF SVM was used as the classifier.

Li *et al.* [94] considered cross-subject EEG emotion classification for both supervised (the target subject has some labeled samples) and semisupervised (the target subject has some labeled samples and unlabeled samples) scenarios. We briefly introduce only their best-performing supervised approach here. Multiple source domains are assumed. They first performed source selection by training a classifier in each source domain and compute its classification accuracy on the labeled samples in the target domain. These accuracies were then sorted to select the top few source subjects. A style transfer mapping was learned between the target and each selected source. For each selected source subject, they performed SVM classification on his/her data, removed the support vectors (because they are near the decision boundary and hence uncertain), performed k -means clustering on the remaining samples to obtain the prototypes, and mapped each target-domain labeled sample feature vector \mathbf{x}_i^n to the nearest prototype in the same class by the following mapping:

$$\min_{A,b} \sum_{i=1}^n \|\mathbf{A}\mathbf{x}_i^n + b - \mathbf{d}_n\|_2^2 + \beta \|A - I\|_F^2 + \gamma \|b\|_2^2 \quad (8)$$

where \mathbf{d}_n is the nearest prototype in the same class of the source domain, and β and γ are hyperparameters. A new, unlabeled sample in the target domain is first mapped to each selected source domain and then classified by a classifier trained in the corresponding source domain. The classification results from all source domains were then weighted averaged, where the weights were determined by the accuracies of the source-domain classifiers.

Deep learning has also been gaining popularity in aBCI.

Chai *et al.* [95] proposed a subspace alignment autoencoder (SAAE) for cross-subject and cross-session transfer in EEG-based emotion classification. First, differential entropy features from both domains were transformed into a domain-invariant subspace using a stacked autoencoder. Then, kernel PCA, graph regularization, and maximum mean discrepancy were used to reduce the feature distribution discrepancy between the two domains. After that, a classifier trained in the source domain can be directly applied to the target domain.

Yin and Zhang [96] proposed an adaptive stacked denoising autoencoder (SDAE) for cross-session binary classification of mental workload levels from EEG. The weights of the shallow hidden neurons of the SDAE were adaptively updated during the testing phase using augmented testing samples and their pseudolabels.

Zheng *et al.* [97] presented EmotionMeter, a multimodal emotion recognition framework that combines brain waves and eye movements to classify four emotions (fear, sadness, happiness, and neutrality). They adopted a bimodal deep autoencoder to extract the shared representations of both EEGs and eye movements. The experimental results demonstrated that modality fusion combining EEG and eye movements with multimodal deep learning can significantly enhance emotion recognition accuracy compared with a single modality. They also investigated the complementary characteristics of EEGs and eye movements for emotion recognition and the stability of EmotionMeter across sessions. They found that EEGs and eye movements have important complementary characteristics, e.g., EEGs have the advantage of classifying happy emotion (80%) compared with eye movements (67%), whereas eye movements outperform EEGs in recognizing fear emotion (67% versus 65%).

Fahimi *et al.* [98] performed cross-subject attention classification. They first trained a CNN by combining EEG data from source subjects and then fine tuned it by using some calibration data from the target subject. The inputs were raw EEGs, bandpass filtered EEGs, and decomposed EEGs (delta, theta, alpha, beta, and gamma bands).

Li *et al.* [99] proposed R2G-STNN, which consists of spatial and temporal neural networks with regional-to-global hierarchical feature learning, to learn discriminative spatial-temporal EEG features for subject-independent emotion classification. To learn the spatial features, a bidirectional long short-term memory (LSTM) network was used to capture the intrinsic spatial relationships of EEG electrodes within and between different brain regions. A region-attention layer was also introduced to learn the weights of different brain regions. A domain discriminator working corporately with the classifier was used to reduce domain shift between training and testing.

Li *et al.* [100] further proposed an improved bihemisphere domain adversarial neural network (BiDANN-S) for subject-independent emotion classification. Inspired by the neuroscience findings that the left and right hemispheres of the human brain are asymmetric to the emotional response, BiDANN-S uses a global and two local domain discriminators working adversarially with a classifier to learn discriminative emotional features for each hemisphere. To improve the generalization performance and to facilitate subject-independent

EEG emotion classification, it also tries to reduce the possible domain differences in each hemisphere between the source and target domains and ensure that the extracted EEG features are robust to subject variations.

Li *et al.* [101] proposed a neural network model for cross-subject/session EEG emotion recognition, which does not require label information in the target domain. The neural network was optimized by minimizing the classification error in the source domain while making the source and target domains similar in their latent representations. Adversarial training was used to adapt the marginal distributions in the early layers, and association reinforcement was performed to adapt the conditional distributions in the last few layers. In this way, it achieved joint distribution adaptation [102].

Song *et al.* [103] proposed a dynamical graph CNN (DGCNN) for subject-dependent and subject-independent emotion classification. Each EEG channel was represented as a node in the DGCNN, and differential entropy features from five frequency bands were used as inputs. After graph filtering, a 1×1 convolution layer learned the discriminative features among the five frequency bands. An ReLU activation function was adopted to ensure that the outputs of the graph filtering layer are nonnegative. The outputs of the activation function were sent to a multilayer dense network for classification.

Appriou *et al.* [104] compared several modern machine learning algorithms on subject-specific and subject-independent cognitive and emotional state classification, including Riemannian approaches and a CNN. They found that CNN performed the best in both subject-specific and subject-independent workload classification. A filter bank tangent space classifier (FBTSC) was also proposed. It first filters an EEG into several different frequency bands. For each band, it computes the covariance matrices of the EEG trials, projects them onto the tangent space at their mean, and then applies a Euclidean space classifier. FBTSC achieved the best performance in subject-specific emotion (valence and arousal) classification.

B. Cross-Device TL

Lan *et al.* [105] considered cross-data set transfers between DEAP and SEED, which have different numbers of subjects, and were recorded using different EEG devices with different numbers of electrodes. They used only three trials (one positive, one neutral, and one negative) from 14 selected subjects in DEAP and only the 32 common channels between the two data sets. Five differential entropy features in five different frequency bands (delta, theta, alpha, beta, and gamma) were extracted from each channel and concatenated as features. Experiments showed that domain adaptation, particularly transfer component analysis [106] and maximum independence domain adaptation [107], can effectively improve the classification accuracies compared to the baseline.

Lin [108] proposed RPCA-embedded TL to generate a personalized cross-day emotion classifier with less labeled data while obviating intraindividual and interindividual differences. The source data set consists of 12 subjects using a 14-channel Emotiv EPOC device, and the target data set consists of 26

different subjects using a 30-channel Neuroscan Quik-Cap. Twelve of the 26 channels of Quik-Cap were first selected to align with 12 of the 14 selected channels from the EPOC device. The Quik-Cap EEG signals were also downsampled and filtered to match those of the EPOC device. Five frequency band (delta, theta, alpha, beta, and gamma) features from each of the six left-right channel pairs (e.g., AF3-AF4, F7-F8), four fronto-posterior pairs (e.g., AF3-O1, F7-P7), and the 12 selected channels were extracted, resulting in a 120-D feature vector for each trial. Similar to [89], the sparse RPCA matrix of the feature matrix was used as the final feature. The Riemannian distance between the trials of each source subject and the target subject was computed as a dissimilarity measure to select the most similar source subjects, whose trials were combined with the trials from the target subject to train an SVM classifier.

Zheng *et al.* [109] considered an interesting cross-device (or cross-modality) and cross-subject TL scenario in which the target subject's eye-tracking data were used to enhance the performance of cross-subject EEG-based affect classification. It is a three-step procedure. First, multiple individual emotion classifiers are trained for the source subjects. Second, a regression function is learned to model the relationship between the data distribution and classifier parameters. Third, a target classifier is constructed using the target feature distribution and distribution-to-classifier mapping. This heterogeneous TL approach achieved comparable performance with homogeneous EEG-based models and scanpath-based models. To the best of our knowledge, this is the first study that transfers between two different types of signals.

Deep learning has also been used in cross-device TL in aBCIs. EEG trials are usually transformed into some sort of images before input to the deep learning model. In this way, EEG signals from different devices can be made consistent.

Siddharth *et al.* [110] performed multimodality (e.g., EEG, ECG, face, etc.) cross-data set emotion classification, e.g., training on DEAP and testing on the MAHNOB-HCI database [111]. We only briefly introduce their EEG-based deep learning approach here, which works for data sets with different numbers and placements of electrodes, different sampling rates, etc. The EEG PSDs in the theta, alpha, and beta bands were used to plot three topographies for each trial. Then, each topography was considered a component of a color image and weighted by the ratio of alpha blending to form the color image. In this way, one color image representing the topographic PSD was obtained for each trial, and the images obtained from different EEG devices can be directly combined or compared. A pretrained VGG-16 network was used to extract 4096 features from each image, whose number was later reduced to 30 by PCA. An extreme learning machine was used as the classifier for the final classification.

Cimtay and Ekmekcioglu [112] used a pretrained state-of-the-art CNN model, Inception-ResNet-v2, for cross-subject and cross-data set transfers. Since Inception-ResNet-v2 requires the input data size to be $(N_1, N, 3)$, where $N_1 \geq 75$ is the number of EEG channels and $N \geq 75$ is the number of time-domain samples, when the number of EEG channels is less than 75, they increased the number of channels by adding

noisy copies of them (Gaussian random noise was used) to reach $N_1 = 80$. This process was repeated three times so that each trial became an $80 \times 300 \times 3$ matrix, which was then used as the input to Inception-ResNet-v2. They also added a global average pooling layer and five dense layers after Inception-ResNet-v2 for classification.

VII. TL IN BCI REGRESSION PROBLEMS

There are many important BCI regression problems, e.g., driver drowsiness estimation [38]–[40], vigilance estimation [11], [12], [113], and user reaction time estimation [41], which were not adequately addressed in previous reviews. This section fills this gap. Because there were no publications on cross-device and cross-task TL in BCI regression problems, we do not have sections on them.

A. Cross-Subject/Session TL

Wu *et al.* [40] proposed a novel online wAR for regression (OwARR) algorithm to reduce the amount of subject-specific calibration data in EEG-based driver drowsiness estimation and a source-domain selection approach to save approximately half of its computational cost. OwARR minimizes the following loss function, similar to wAR [26]:

$$\begin{aligned} \min_f \sum_{n=1}^{N_s} (y_s^n - f(X_s^n))^2 + w_t \sum_{n=1}^{N_t} (y_t^n - f(X_t^n))^2 \\ + \lambda [d(P_s(X_s), P_t(X_t)) + d(P_s(X_s|y_s), P_t(X_t|y_t))] \\ - \gamma \tilde{r}^2(y, f(X)) \end{aligned} \quad (9)$$

where λ and γ are nonnegative regularization parameters and w_t is the overall weight for target domain samples. $\tilde{r}^2(y, f(X))$ approximates the sample Pearson correlation coefficient between y and $f(X)$. Fuzzy sets were used to define fuzzy classes so that $d(P_s(X_s|y_s), P_t(X_t|y_t))$ can be efficiently computed. The five terms in (9) minimize the fitting error in the source domain, the fitting error in the target domain, the distance between the marginal probability distributions, the distance between the conditional probability distributions, and the estimated sample Pearson correlation coefficient between y and $f(X)$. Wu *et al.* [40] showed that OwARR and OwARR with source-domain selection can achieve significantly smaller estimation errors than several other cross-subject TL approaches.

Jiang *et al.* [39] further extended OwARR to multiview learning, where the first view included theta band powers from all channels and the second view converted the first view into dBs and removed some bad channels. A TSK fuzzy system was used as the regression model, optimized by minimizing (9) for both views simultaneously and adding an additional term to enforce the consistency between the two views (the estimation from one view should be close to that from the other view). They demonstrated that the proposed approach outperformed a domain adaptation with a model fusion approach [114] in cross-subject TL.

Wei *et al.* [115] also performed cross-subject driver drowsiness estimation. Their procedure consisted of three steps.

- 1) *Ranking*: For each source subject, it computed six distance measures (Euclidean distance, correlation distance, Chebyshev distance, cosine distance, Kullback–Leibler divergence, and transferability-based distance) between his/her own alert baseline (the first ten trials) power distribution and all other source subjects' distributions and the cross-subject model performance (XP), which is the transferability of other source subjects on the current subject. A support vector regression (SVR) model was then trained to predict XP from distance measures. In this way, given a target subject with a few calibration trials, the XP of the source subjects can be computed and ranked.
- 2) *Fusion*: A weighted average was used to combine the source models, where the weights were determined from a modified logistic function optimized on the source subjects.
- 3) *Recalibration*: The weighted average was subtracted by an offset, estimated as the median of the initial ten calibration trials (i.e., the alert baseline) from the target subject. They showed that this approach can result in a 90% calibration time reduction in driver drowsiness index estimation.

Chen *et al.* [116] integrated feature selection and an adaptation regularization-based TL (ARTL) [48] classifier for cross-subject driver status classification. The most novel part is feature selection, which extends the traditional ReliefF [88] and minimum redundancy maximum relevancy (mRMR) [117] to class separation and domain fusion (CSDF)-ReliefF and CSDF-mRMR, which consider both the class separability and the domain similarity, i.e., the selected feature subset should simultaneously maximize the distinction among different classes and minimize the difference among different domains. The ranks of the features from different feature selection algorithms were then fused to identify the best feature set, which was used in ARTL for classification.

Deep learning has also been used in BCI regression problems.

Ming *et al.* [118] proposed a stacked differentiable neural computer and demonstrated its effectiveness in cross-subject EEG-based mind load estimation and reaction time estimation. The original LSTM network controller in differentiable neural computers was replaced by a recurrent convolutional network controller, and the memory-accessing structures were also adjusted for processing EEG topographic data.

Cui *et al.* [38] proposed a subject-independent TL approach, feature weighted episodic training (FWET), to completely eliminate the calibration requirement in cross-subject transfers in EEG-based driver drowsiness estimation. It integrates feature weighting to learn the importance of different features and episodic training for domain generalization. Episodic training considers the conditional distributions $P(y_s|f(X_s))$ directly and trains a regression network f that aligns $P(y_s|f(X_s))$ in all the source domains, which usually generalizes well to the unseen target domain \mathcal{D}_t . It first establishes a subject-specific feature transformation model f_{θ_s} and a subject-specific regression model f_{ψ_s} for each source subject to learn the domain-specific information, then trains a feature transformation model f_{θ} that

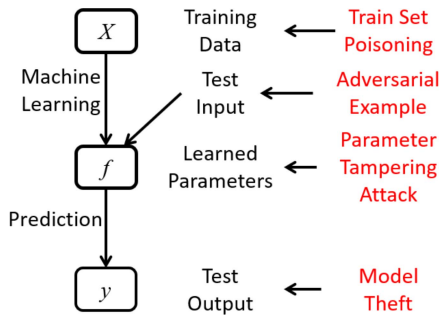


Fig. 3. Attack strategies to different components of a machine learning model.

makes the transformed features from subject s still perform well when applied to a regressor f_{ψ_j} trained on subject j ($j \neq s$). The overall loss function of episodic training, when subject s 's data are fed into subject j 's regressor, is:

$$\begin{aligned} \ell_{s,j} = & \sum_{n=1}^{N_s} \ell(y_s^n, f_{\psi}(f_{\theta}(X_s^n))) \\ & + \lambda \sum_{n=1}^{N_s} \ell(y_s^n, \bar{f}_{\psi_j}(f_{\theta}(X_s^n))) \end{aligned} \quad (10)$$

where \bar{f}_{ψ_j} means that f_{ψ_j} is not updated during backpropagation. Once the optimal f_{ψ} and f_{θ} are obtained, the prediction for X_t is $\hat{y}_t = f_{\psi}(f_{\theta}(X_t))$.

VIII. TL IN ADVERSARIAL ATTACKS OF EEG-BASED BCIs

Adversarial attacks of EEG-based BCIs represent one of the latest developments in BCIs. It was first studied by Zhang and Wu [42]. They found that adversarial perturbations, which are deliberately designed tiny perturbations, can be added to normal EEG trials to fool the machine learning model and cause dramatic performance degradation. Both traditional machine learning models and deep learning models, as well as both classifiers and regression models in EEG-based BCIs, can be attacked.

Adversarial attacks can target different components of a machine learning model, e.g., training data, model parameters, test data, and test output, as shown in Fig. 3. To date, only adversarial examples (benign examples contaminated by adversarial perturbations) targeting the test inputs have been investigated in EEG-based BCIs, so this section only considers adversarial examples.

A more detailed illustration of the adversarial example attack scheme is shown in Fig. 4. A jamming module is injected between signal processing and machine learning to generate adversarial examples.

Table II shows the three attack types in EEG-based BCIs. White-box attacks know all information about the victim model, including its architecture and parameters, and hence are the easiest to perform. Black-box attacks know nothing about the victim model but can only supply inputs to it and observe its output and hence are the most challenging to perform.

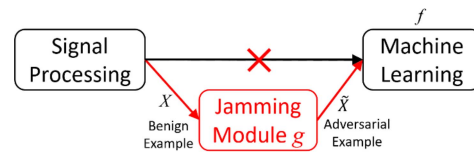


Fig. 4. Adversarial example generation scheme [42].

TABLE II
SUMMARY OF THE THREE ATTACK TYPES IN EEG-BASED BCIs [42]

Victim Model Information	White-Box Attacks	Grey-Box Attacks	Black-Box Attacks
Know its architecture	✓	×	×
Know its parameters θ	✓	×	×
Know its training data	—	✓	×
Can observe its response	—	—	✓

A. Cross-Model Attacks

Different from the cross-subject/session/device/task TL scenarios considered in the previous five sections, adversarial attacks in BCIs so far mainly considered cross-model attacks,² where adversarial examples generated from one machine learning model are used to attack another model. This assumption is necessary for gray-box and black-box attacks because the victim model is unknown, and the attacker needs to construct its own model (called the substitute model) to approximate the victim model.

Interestingly, cross-model attacks can be performed without explicitly considering TL. They are usually achieved by making use of the transferability of adversarial examples [119], i.e., adversarial examples generated by one machine learning model may also be used to fool a different model. The fundamental reason behind this property is still unclear, but it does not hinder people from making use of it.

For example, Zhang and Wu [42] proposed unsupervised fast gradient sign methods, which can effectively perform white-box, gray-box, and black-box attacks on deep learning classifiers. Two BCI paradigms, i.e., MI and ERP, and three popular deep learning models, i.e., EEGNet, Deep ConvNet, and Shallow ConvNet, were considered. Meng *et al.* [43] further showed that the transferability of adversarial examples can also be used to attack regression models in BCIs; e.g., adversarial examples designed from a multilayer perceptron neural network can be used to attack a ridge regression model, and *vice versa*, in EEG-based user reaction time estimation.

IX. CONCLUSION

This article has reviewed recently proposed TL approaches in EEG-based BCIs, according to six different paradigms and applications: 1) MI; 2) ERP; 3) SSVEP; 4) aBCI; 5) regression problems; and 6) adversarial attacks. TL algorithms are

²Existing publications [42], [43] also considered *cross-subject* attacks, but the meaning of cross-subject in adversarial attacks is different from the cross-subject TL setting in previous sections: in adversarial attacks, cross-subject means that the same machine learning model is used by all subjects, but the scheme for generating adversarial examples is designed on some subjects and applied to another subject. It assumes that the victim machine learning model works well for all subjects.

grouped into cross-subject/session, cross-device, and cross-task approaches and introduced separately. Connections among similar approaches are also pointed out.

The following observations and conclusions can be made, which may point to some future research directions.

- 1) Among the three classic BCI paradigms (MI, ERP, and SSVEP), SSVEP seems to receive the least amount of attention. Very few TL approaches have been proposed recently. One reason may be that MI and ERP are very similar, so many TL approaches developed for MI can be applied to ERPs directly or with little modification, e.g., RA, EA, RPA, and EEGNet, whereas SSVEP is a quite different paradigm.
- 2) Two new applications of EEG-based BCIs, i.e., aBCI and regression problems, have been attracting increasing research interest. Interestingly, both of them are passive BCIs [120]. Although both classification and regression problems can be formulated in aBCIs, existing research has focused almost exclusively on classification problems.
- 3) Adversarial attacks, one of the latest developments in EEG-based BCIs, can be performed across different machine learning models by utilizing the transferability of adversarial examples. However, explicitly considering TL between different domains may further improve the attack performance. For example, in black-box attacks, TL can make use of publicly available data sets to reduce the number of queries to the victim model or, in other words, to better approximate the victim model given the same number of queries.
- 4) Most TL studies focused on cross-subject/session transfers. Cross-device transfers have started to attract attention, but cross-task transfers remain largely unexplored. To the best of our knowledge, there has been only one such study [50] since 2016. Effective cross-device and cross-task transfers would make EEG-based BCIs much more practical.
- 5) Among various TL approaches, Riemannian geometry and deep learning are emerging and gaining momentum, each of which has a group of approaches proposed.
- 6) Although most research on TL in BCIs has focused on classifiers or regression models, i.e., at the pattern recognition stage, TL in BCIs can also be performed in trial alignment, e.g., RA, EA, LA, and RPA, in signal filtering, e.g., transfer kernel CSPs [51], and in feature extraction/selection, e.g., CSDF-ReliefF and CSDF-mRMR [116]. Additionally, these TL-based individual components can also be assembled into a complete machine learning pipeline to achieve even better performance. For example, EA and LA data alignment schemes have been combined with TL classifiers [50], [60], and CSDF-ReliefF and CSDF-mRMR feature selection approaches have also been integrated with TL classifiers [116].
- 7) TL can also be integrated with other machine learning approaches, e.g., active learning [24], for improved performance [25], [26].

REFERENCES

- [1] J. R. Wolpaw, N. Birbaumer, D. J. McFarland, G. Pfurtscheller, and T. M. Vaughan, "Brain-computer interfaces for communication and control," *Clin. Neurophysiol.*, vol. 113, no. 6, pp. 767–791, 2002.
- [2] B. J. Lance, S. E. Kerick, A. J. Ries, K. S. Oie, and K. McDowell, "Brain-computer interface technologies in the coming decades," *Proc. IEEE*, vol. 100, no. 3, pp. 1585–1599, 2012.
- [3] J. J. Vidal, "Toward direct brain-computer communication," *Annu. Rev. Biophys. Bioeng.*, vol. 2, no. 1, pp. 157–180, 1973.
- [4] E. E. Fetz, "Operant conditioning of cortical unit activity," *Science*, vol. 163, no. 3870, pp. 955–958, 1969.
- [5] J. M. R. Delgado, *Physical Control of the Mind: Toward a Psychocivilized Society*, vol. 41. New York, NY, USA: World Bank, 1969.
- [6] G. Pfurtscheller, G. R. Müller-Putz, R. Scherer, and C. Neuper, "Rehabilitation with brain-computer interface systems," *Computer*, vol. 41, no. 10, pp. 58–65, 2008.
- [7] J. van Erp, F. Lotte, and M. Tangermann, "Brain-computer interfaces: Beyond medical applications," *Computer*, vol. 45, no. 4, pp. 26–34, 2012.
- [8] D. Marshall, D. Coyle, S. Wilson, and M. Callaghan, "Games, game-play, and BCI: The state of the art," *IEEE Trans. Comput. Intell. AI Games*, vol. 5, no. 2, pp. 82–99, Jun. 2013.
- [9] W.-L. Zheng and B.-L. Lu, "Investigating critical frequency bands and channels for EEG-based emotion recognition with deep neural networks," *IEEE Trans. Auton. Mental Develop.*, vol. 7, no. 3, pp. 162–175, Sep. 2015.
- [10] T. G. Monteiro, C. Skourup, and H. Zhang, "Using EEG for mental fatigue assessment: A comprehensive look into the current state of the art," *IEEE Trans. Human-Mach. Syst.*, vol. 49, no. 6, pp. 599–610, Dec. 2019.
- [11] W.-L. Zheng and B.-L. Lu, "A multimodal approach to estimating vigilance using EEG and forehead EOG," *J. Neural Eng.*, vol. 14, no. 2, 2017, Art. no. 026017.
- [12] L.-C. Shi and B.-L. Lu, "EEG-based vigilance estimation using extreme learning machines," *Neurocomputing*, vol. 102, pp. 135–143, Feb. 2013.
- [13] R. P. Rao, *Brain-Computer Interfacing: An Introduction*. New York, NY, USA: Cambridge Univ. Press, 2013.
- [14] L.-D. Liao *et al.*, "Biosensor technologies for augmented brain-computer interfaces in the next decades," *Proc. IEEE*, vol. 100, no. 2, pp. 1553–1566, 2012.
- [15] S. Makeig, C. Kothe, T. Mullen, N. Bigdely-Shamlo, Z. Zhang, and K. Kreutz-Delgado, "Evolving signal processing for brain-computer interfaces," *Proc. IEEE*, vol. 100, pp. 1567–1584, May 2012.
- [16] H. Ramoser, J. Müller-Gerking, and G. Pfurtscheller, "Optimal spatial filtering of single trial EEG during imagined hand movement," *IEEE Trans. Rehabil. Eng.*, vol. 8, no. 4, pp. 441–446, Dec. 2000.
- [17] S. Makeig, A. J. Bell, T.-P. Jung, and T. J. Sejnowski, "Independent component analysis of electroencephalographic data," in *Proc. Adv. Neural Inf. Process. Syst.*, Denver, CO, USA, Dec. 1996, pp. 145–151.
- [18] T.-P. Jung *et al.*, "Removing electroencephalographic artifacts by blind source separation," *Psychophysiology*, vol. 37, no. 2, pp. 163–178, 2000.
- [19] B. Rivet, A. Souloumiac, V. Attina, and G. Gibert, "xDAWN algorithm to enhance evoked potentials: Application to brain-computer interface," *IEEE Trans. Biomed. Eng.*, vol. 56, no. 8, pp. 2035–2043, Aug. 2009.
- [20] X.-W. Wang, D. Nie, and B.-L. Lu, "Emotional state classification from EEG data using machine learning approach," *Neurocomputing*, vol. 129, pp. 94–106, Apr. 2014.
- [21] F. Yger, M. Berar, and F. Lotte, "Riemannian approaches in brain-computer interfaces: A review," *IEEE Trans. Neural Syst. Rehabil. Eng.*, vol. 25, no. 10, pp. 1753–1762, Oct. 2017.
- [22] X. Wu, W.-L. Zheng, and B.-L. Lu, "Identifying functional brain connectivity patterns for EEG-based emotion recognition," in *Proc. 9th Int. IEEE/EMBS Conf. Neural Eng.*, San Francisco, CA, USA, Mar. 2019, pp. 235–238.
- [23] S. J. Pan and Q. Yang, "A survey on transfer learning," *IEEE Trans. Knowl. Data Eng.*, vol. 22, no. 10, pp. 1345–1359, Oct. 2010.
- [24] B. Settles, "Active learning literature survey," *Comput. Sci., Univ. Wisconsin-Madison, Rep.* 1648, 2009.
- [25] D. Wu, B. J. Lance, and T. D. Parsons, "Collaborative filtering for brain-computer interaction using transfer learning and active class selection," *PLoS ONE*, vol. 8, no. 2, 2013, Art. no. e56624.

- [26] D. Wu, V. J. Lawhern, W. D. Hairston, and B. J. Lance, "Switching EEG headsets made easy: Reducing offline calibration effort using active weighted adaptation regularization," *IEEE Trans. Neural Syst. Rehabil. Eng.*, vol. 24, no. 11, pp. 1125–1137, Nov. 2016.
- [27] G. Pfurtscheller and C. Neuper, "Motor imagery and direct brain-computer communication," *Proc. IEEE*, vol. 89, no. 7, pp. 1123–1134, 2001.
- [28] T. C. Handy, Ed., *Event-Related Potentials: A Methods Handbook*. Boston, MA, USA: MIT Press, 2005.
- [29] S. Lees *et al.*, "A review of rapid serial visual presentation-based brain-computer interfaces," *J. Neural Eng.*, vol. 15, no. 2, 2018, Art. no. 021001.
- [30] S. Sutton, M. Braren, J. Zubin, and E. John, "Evoked-potential correlates of stimulus uncertainty," *Science*, vol. 150, no. 3700, pp. 1187–1188, 1965.
- [31] O. Friman, I. Volosyay, and A. Graser, "Multiple channel detection of steady-state visual evoked potentials for brain-computer interfaces," *IEEE Trans. Biomed. Eng.*, vol. 54, no. 4, pp. 742–750, Apr. 2007.
- [32] F. Beverina *et al.*, "User adaptive BCIs: SSVEP and P300 based interfaces," *Psychol. J.*, vol. 1, no. 4, pp. 331–354, 2003.
- [33] X. Chen, Y. Wang, M. Nakanishi, X. Gao, T.-P. Jung, and S. Gao, "High-speed spelling with a noninvasive brain-computer interface," *Proc. Nat. Acad. Sci. USA*, vol. 112, no. 44, pp. E6058–E6067, 2015.
- [34] C. Muhl, B. Allison, A. Nijholt, and G. Chanel, "A survey of affective brain computer interfaces: Principles, state-of-the-art, and challenges," *Brain-Comput. Interfaces*, vol. 1, no. 2, pp. 66–84, 2014.
- [35] A. Al-Nafjan, M. Hosny, Y. Al-Ohali, and A. Al-Wabil, "Review and classification of emotion recognition based on EEG brain-computer interface system research: A systematic review," *Appl. Sci.*, vol. 7, no. 12, p. 1239, 2017.
- [36] Y.-W. Shen and Y.-P. Lin, "Challenge for affective brain-computer interfaces: Non-stationary spatio-spectral EEG oscillations of emotional responses," *Front. Human Neurosci.*, vol. 13, p. 366, Oct. 2019.
- [37] S. M. Alarcao and M. J. Fonseca, "Emotions recognition using EEG signals: A survey," *IEEE Trans. Affect. Comput.*, vol. 10, no. 3, pp. 374–393, Jul.–Sep. 2019.
- [38] Y. Cui, Y. Xu, and D. Wu, "EEG-based driver drowsiness estimation using feature weighted episodic training," *IEEE Trans. Neural Syst. Rehabil. Eng.*, vol. 27, no. 11, pp. 2263–2273, Sep. 2019.
- [39] Y. Jiang, Y. Zhang, C. Lin, D. Wu, and C.-T. Lin, "EEG-based driver drowsiness estimation using an online multi-view and transfer TSK fuzzy system," *IEEE Trans. Intell. Transp. Syst.*, early access, Feb. 27, 2020, doi: [10.1109/ITITS.2020.2973673](https://doi.org/10.1109/ITITS.2020.2973673).
- [40] D. Wu, V. J. Lawhern, S. Gordon, B. J. Lance, and C.-T. Lin, "Driver drowsiness estimation from EEG signals using online weighted adaptation regularization for regression (OwARR)," *IEEE Trans. Fuzzy Syst.*, vol. 25, no. 6, pp. 1522–1535, Dec. 2017.
- [41] D. Wu, V. J. Lawhern, B. J. Lance, S. Gordon, T.-P. Jung, and C.-T. Lin, "EEG-based user reaction time estimation using Riemannian geometry features," *IEEE Trans. Neural Syst. Rehabil. Eng.*, vol. 25, no. 11, pp. 2157–2168, Nov. 2017.
- [42] X. Zhang and D. Wu, "On the vulnerability of CNN classifiers in EEG-based BCIs," *IEEE Trans. Neural Syst. Rehabil. Eng.*, vol. 27, no. 5, pp. 814–825, May 2019.
- [43] L. Meng, C.-T. Lin, T.-P. Jung, and D. Wu, "White-box target attack for EEG-based BCI regression problems," in *Proc. Int. Conf. Neural Inf. Process.*, Dec. 2019, pp. 476–488.
- [44] P. Wang, J. Lu, B. Zhang, and Z. Tang, "A review on transfer learning for brain-computer interface classification," in *Proc. 5th Int. Conf. Inf. Sci. Technol.*, Changsha, China, Apr. 2015, pp. 1318–1324.
- [45] V. Jayaram, M. Alamgir, Y. Altun, B. Scholkopf, and M. Grosse-Wentrup, "Transfer learning in brain-computer interfaces," *IEEE Comput. Intell. Mag.*, vol. 11, no. 1, pp. 20–31, Dec. 2016.
- [46] F. Lotte *et al.*, "A review of classification algorithms for EEG-based brain-computer interfaces: A 10 year update," *J. Neural Eng.*, vol. 15, no. 3, 2018, Art. no. 031005.
- [47] A. M. Azab, J. Toth, L. S. Mihaylova, and M. Arvaneh, "A review on transfer learning approaches in brain-computer interface," in *Signal Processing and Machine Learning for Brain-Machine Interfaces*, T. Tanaka and M. Arvaneh, Eds. Berlin, Germany: Inst. Eng. Technol., 2018, pp. 81–98.
- [48] M. Long, J. Wang, G. Ding, S. J. Pan, and P. S. Yu, "Adaptation regularization: A general framework for transfer learning," *IEEE Trans. Knowl. Data Eng.*, vol. 26, no. 5, pp. 1076–1089, May 2014.
- [49] Y. Zhang and Q. Yang, "An overview of multi-task learning," *Nat. Sci. Rev.*, vol. 5, no. 1, pp. 30–43, 2018.
- [50] H. He and D. Wu, "Different set domain adaptation for brain-computer interfaces: A label alignment approach," *IEEE Trans. Neural Syst. Rehabil. Eng.*, vol. 28, no. 5, pp. 1091–1108, May 2020.
- [51] M. Dai, D. Zheng, S. Liu, and P. Zhang, "Transfer kernel common spatial patterns for motor imagery brain-computer interface classification," *Comput. Math. Methods Med.*, Mar. 2018, Art. no. 9871603.
- [52] H. Albalawi and X. Song, "A study of kernel CSP-based motor imagery brain computer interface classification," in *Proc. IEEE Signal Process. Med. Biol. Symp.*, New York, NY, USA, Dec. 2012, pp. 1–4.
- [53] M. Long, J. Wang, J. Sun, and S. Y. Philip, "Domain invariant transfer kernel learning," *IEEE Trans. Knowl. Data Eng.*, vol. 27, no. 6, pp. 1519–1532, Jun. 2015.
- [54] A. M. Azab, L. Mihaylova, K. K. Ang, and M. Arvaneh, "Weighted transfer learning for improving motor imagery-based brain-computer interface," *IEEE Trans. Neural Syst. Rehabil. Eng.*, vol. 27, no. 7, pp. 1352–1359, Jul. 2019.
- [55] I. Hossain, A. Khosravi, I. Hettiarachchi, and S. Nahavandi, "Multiclass informative instance transfer learning framework for motor imagery-based brain-computer interface," *Comput. Intell. Neurosci.*, Feb. 2018, Art. no. 6323414.
- [56] D. Wu, B. J. Lance, and V. J. Lawhern, "Transfer learning and active transfer learning for reducing calibration data in single-trial classification of visually evoked potentials," in *Proc. IEEE Int. Conf. Syst. Man Cybern.*, San Diego, CA, USA, Oct. 2014, pp. 2801–2807.
- [57] P. Zanini, M. Congedo, C. Jutten, S. Said, and Y. Berthoumieu, "Transfer learning: A Riemannian geometry framework with applications to brain-computer interfaces," *IEEE Trans. Biomed. Eng.*, vol. 65, no. 5, pp. 1107–1116, May 2018.
- [58] A. Barachant, S. Bonnet, M. Congedo, and C. Jutten, "Multiclass brain-computer interface classification by Riemannian geometry," *IEEE Trans. Biomed. Eng.*, vol. 59, no. 4, pp. 920–928, Apr. 2012.
- [59] O. Yair, M. Ben-Chen, and R. Talmon, "Parallel transport on the cone manifold of SPD matrices for domain adaptation," *IEEE Trans. Signal Process.*, vol. 67, no. 7, pp. 1797–1811, Jan. 2019.
- [60] H. He and D. Wu, "Transfer learning for brain-computer interfaces: A Euclidean space data alignment approach," *IEEE Trans. Biomed. Eng.*, vol. 67, no. 2, pp. 399–410, Feb. 2020.
- [61] P. L. C. Rodrigues, C. Jutten, and M. Congedo, "Riemannian procrustes analysis: Transfer learning for brain-computer interfaces," *IEEE Trans. Biomed. Eng.*, vol. 66, no. 8, pp. 2390–2401, Aug. 2019.
- [62] W. Zhang and D. Wu, "Manifold embedded knowledge transfer for brain-computer interfaces," *IEEE Trans. Neural Syst. Rehabil. Eng.*, vol. 28, no. 5, pp. 1117–1127, May 2020.
- [63] A. Singh, S. Lal, and H. W. Guesgen, "Small sample motor imagery classification using regularized Riemannian features," *IEEE Access*, vol. 7, pp. 46858–46869, 2019.
- [64] A. Barachant, S. Bonnet, M. Congedo, and C. Jutten, "Riemannian geometry applied to BCI classification," in *Proc. Int. Conf. Latent Variable Anal. Signal Separation*, St. Malo, France, Sep. 2010, pp. 629–636.
- [65] R. T. Schirmermeister *et al.*, "Deep learning with convolutional neural networks for EEG decoding and visualization," *Human Brain Map.*, vol. 38, no. 11, pp. 5391–5420, 2017.
- [66] K. K. Ang, Z. Y. Chin, H. Zhang, and C. Guan, "Filter bank common spatial pattern (FBCSP) in brain-computer interface," in *Proc. IEEE World Congr. Comput. Intell.*, Hong Kong, Jun. 2008, pp. 2390–2397.
- [67] V. J. Lawhern, A. J. Solon, N. R. Waytowich, S. M. Gordon, C. P. Hung, and B. J. Lance, "EEGNet: A compact convolutional neural network for EEG-based brain-computer interfaces," *J. Neural Eng.*, vol. 15, no. 5, 2018, Art. no. 056013.
- [68] Y.-X. Wang, D. Ramanan, and M. Hebert, "Growing a brain: Fine-tuning by increasing model capacity," in *Proc. IEEE Conf. Comput. Vis. Pattern Recognit.*, Honolulu, HI, USA, Jul. 2017, pp. 2471–2480.
- [69] C.-S. Wei, T. Koike-Akino, and Y. Wang, "Spatial component-wise convolutional network (SCCNet) for motor-imagery EEG classification," in *Proc. 9th IEEE/EMBS Int. Conf. Neural Eng.*, San Francisco, CA, USA, Mar. 2019, pp. 328–331.
- [70] H. Wu *et al.*, "A parallel multiscale filter bank convolutional neural networks for motor imagery EEG classification," *Front. Neurosci.*, vol. 13, p. 1275, Nov. 2019.
- [71] L. Xu, M. Xu, Y. Ke, X. An, S. Liu, and D. Ming, "Cross-dataset variability problem in EEG decoding with deep learning," *Front. Human Neurosci.*, vol. 14, p. 103, Apr. 2020.
- [72] N. R. Waytowich, V. J. Lawhern, A. W. Bohannon, K. R. Ball, and B. J. Lance, "Spectral transfer learning using information geometry for a user-independent brain-computer interface," *Front. Neurosci.*, vol. 10, p. 430, Sep. 2016.

- [73] F. Parisi, F. Strino, B. Nadler, and Y. Kluger, "Ranking and combining multiple predictors without labeled data," *Proc. Nat. Acad. Sci. USA*, vol. 111, no. 4, pp. 1253–1258, 2014.
- [74] D. Wu, "Online and offline domain adaptation for reducing BCI calibration effort," *IEEE Trans. Human-Mach. Syst.*, vol. 47, no. 4, pp. 550–563, Aug. 2017.
- [75] H. Qi, Y. Xue, L. Xu, Y. Cao, and X. Jiao, "A speedy calibration method using Riemannian geometry measurement and other-subject samples on a P300 speller," *IEEE Trans. Neural Syst. Rehabil. Eng.*, vol. 26, no. 3, pp. 602–608, Mar. 2018.
- [76] J. Jin *et al.*, "The study of generic model set for reducing calibration time in P300-based brain-computer interface," *IEEE Trans. Neural Syst. Rehabil. Eng.*, vol. 28, no. 1, pp. 3–12, Jan. 2020.
- [77] I. J. Goodfellow *et al.*, "Generative adversarial nets," in *Proc. Adv. Neural Inf. Process. Syst.*, Dec. 2014, pp. 2672–2680.
- [78] Y. Ming *et al.*, "Subject adaptation network for EEG data analysis," *Appl. Soft Comput.*, vol. 84, Nov. 2019, Art. no. 105689.
- [79] N. Waytowich *et al.*, "Compact convolutional neural networks for classification of asynchronous steady-state visual evoked potentials," *J. Neural Eng.*, vol. 15, no. 6, 2018, Art. no. 066031.
- [80] M. Nakanishi, Y. Wang, C. Wei, K. Chiang, and T. Jung, "Facilitating calibration in high-speed BCI spellers via leveraging cross-device shared latent responses," *IEEE Trans. Biomed. Eng.*, vol. 67, no. 4, pp. 1105–1113, Apr. 2020.
- [81] P. Ekman and W. Friesen, "Constants across cultures in the face and emotion," *J. Pers. Soc. Psychol.*, vol. 17, no. 2, pp. 124–129, 1971.
- [82] J. Russell, "A circumplex model of affect," *J. Pers. Soc. Psychol.*, vol. 39, no. 6, pp. 1161–1178, 1980.
- [83] A. Mehrabian, *Basic Dimensions for a General Psychological Theory: Implications for Personality, Social, Environmental, and Developmental Studies*. Cambridge, U.K.: Oelgeschlager, 1980.
- [84] S. Koelstra *et al.*, "DEAP: A database for emotion analysis using physiological signals," *IEEE Trans. Affect. Comput.*, vol. 3, no. 1, pp. 18–31, Jan.–Mar. 2012.
- [85] W.-L. Zheng, J.-Y. Zhu, and B.-L. Lu, "Identifying stable patterns over time for emotion recognition from EEG," *IEEE Trans. Affect. Comput.*, vol. 10, no. 3, pp. 417–429, Jul./Sep. 2019.
- [86] X. Chai *et al.*, "A fast, efficient domain adaptation technique for cross-domain electroencephalography (EEG)-based emotion recognition," *Sensors*, vol. 17, no. 5, p. 1014, 2017.
- [87] Y.-P. Lin and T.-P. Jung, "Improving EEG-based emotion classification using conditional transfer learning," *Front. Human Neurosci.*, vol. 11, p. 334, Jun. 2017.
- [88] I. Kononenko, "Estimating attributes: Analysis and extensions of RELIEF," in *Proc. Eur. Conf. Mach. Learn.*, Catania, Italy, Apr. 1994, pp. 171–182.
- [89] Y.-P. Lin, P.-K. Jao, and Y.-H. Yang, "Improving cross-day EEG-based emotion classification using robust principal component analysis," *Front. Comput. Neurosci.*, vol. 11, p. 64, Jun. 2017.
- [90] E. J. Candes, X. Li, Y. Ma, and J. Wright, "Robust principal component analysis?" *J. ACM*, vol. 58, no. 3, p. 11, 2011.
- [91] X. Li, D. Song, P. Zhang, Y. Zhang, Y. Hou, and B. Hu, "Exploring EEG features in cross-subject emotion recognition," *Front. Neurosci.*, vol. 12, p. 162, Mar. 2018.
- [92] S. Liu *et al.*, "Incorporation of multiple-days information to improve the generalization of EEG-based emotion recognition over time," *Front. Human Neurosci.*, vol. 12, p. 267, Jun. 2018.
- [93] F. Yang, X. Zhao, W. Jiang, P. Gao, and G. Liu, "Multi-method fusion of cross-subject emotion recognition based on high-dimensional EEG features," *Front. Comput. Neurosci.*, vol. 13, p. 53, Aug. 2019.
- [94] J. Li, S. Qiu, Y.-Y. Shen, C.-L. Liu, and H. He, "Multisource transfer learning for cross-subject EEG emotion recognition," *IEEE Trans. Cybern.*, vol. 50, no. 7, pp. 3281–3293, Jul. 2020.
- [95] X. Chai, Q. Wang, Y. Zhao, X. Liu, O. Bai, and Y. Li, "Unsupervised domain adaptation techniques based on auto-encoder for non-stationary EEG-based emotion recognition," *Comput. Biol. Med.*, vol. 79, pp. 205–214, Dec. 2016.
- [96] Z. Yin and J. Zhang, "Cross-session classification of mental workload levels using EEG and an adaptive deep learning model," *Biomed. Signal Process. Control*, vol. 33, pp. 30–47, Mar. 2017.
- [97] W.-L. Zheng, W. Liu, Y. Lu, B.-L. Lu, and A. Cichocki, "EmotionMeter: A multimodal framework for recognizing human emotions," *IEEE Trans. Cybern.*, vol. 49, no. 3, pp. 1110–1122, Mar. 2019.
- [98] F. Fahimi, Z. Zhang, W. B. Goh, T.-S. Lee, K. K. Ang, and C. Guan, "Inter-subject transfer learning with an end-to-end deep convolutional neural network for EEG-based BCI," *J. Neural Eng.*, vol. 16, no. 2, 2019, Art. no. 026007.
- [99] Y. Li, W. Zheng, L. Wang, Y. Zong, and Z. Cui, "From regional to global brain: A novel hierarchical spatial-temporal neural network model for EEG emotion recognition," *IEEE Trans. Affect. Comput.*, early access, Jun. 14, 2019, doi: [10.1109/TAFFC.2019.2922912](https://doi.org/10.1109/TAFFC.2019.2922912).
- [100] Y. Li, W. Zheng, Y. Zong, Z. Cui, T. Zhang, and X. Zhou, "A bi-hemisphere domain adversarial neural network model for EEG emotion recognition," *IEEE Trans. Affect. Comput.*, early access, Dec. 7, 2018, doi: [10.1109/TAFFC.2018.2885474](https://doi.org/10.1109/TAFFC.2018.2885474).
- [101] J. Li, S. Qiu, C. Du, Y. Wang, and H. He, "Domain adaptation for EEG emotion recognition based on latent representation similarity," *IEEE Trans. Cogn. Develop. Syst.*, vol. 12, no. 2, pp. 344–353, Jun. 2020.
- [102] M. Long, J. Wang, G. Ding, J. Sun, and P. S. Yu, "Transfer feature learning with joint distribution adaptation," in *Proc. IEEE Int. Conf. Comput. Vis.*, Sydney, NSW, Australia, Dec. 2013, pp. 2200–2207.
- [103] T. Song, W. Zheng, P. Song, and Z. Cui, "EEG emotion recognition using dynamical graph convolutional neural networks," *IEEE Trans. Affect. Comput.*, early access, Mar. 21, 2018, doi: [10.1109/TAFFC.2018.2817622](https://doi.org/10.1109/TAFFC.2018.2817622).
- [104] A. Appriou, A. Cichocki, and F. Lotte, "Modern machine learning algorithms to classify cognitive and affective states from electroencephalography signals," *IEEE Trans. Syst., Man, Cybern., Syst.*, early access.
- [105] Z. Lan, O. Sourina, L. Wang, R. Scherer, and G. R. Muller-Putz, "Domain adaptation techniques for EEG-based emotion recognition: A comparative study on two public datasets," *IEEE Trans. Cogn. Develop. Syst.*, vol. 11, no. 1, pp. 85–94, Mar. 2019.
- [106] S. J. Pan, I. W. Tsang, J. T. Kwok, and Q. Yang, "Domain adaptation via transfer component analysis," *IEEE Trans. Neural Netw.*, vol. 22, no. 2, pp. 199–210, Feb. 2011.
- [107] K. Yan, L. Kou, and D. Zhang, "Learning domain-invariant subspace using domain features and independence maximization," *IEEE Trans. Cybern.*, vol. 48, no. 1, pp. 288–299, Jan. 2018.
- [108] Y. Lin, "Constructing a personalized cross-day EEG-based emotion-classification model using transfer learning," *IEEE J. Biomed. Health Informat.*, vol. 24, no. 5, pp. 1255–1264, May 2020.
- [109] W.-L. Zheng, Z.-F. Shi, and B.-L. Lu, "Building cross-subject EEG-based affective models using heterogeneous transfer learning," *Chin. J. Comput.*, vol. 43, no. 2, pp. 177–189, 2020.
- [110] S. Siddharth, T. Jung, and T. J. Sejnowski, "Utilizing deep learning towards multi-modal bio-sensing and vision-based affective computing," *IEEE Trans. Affect. Comput.*, early access.
- [111] M. Soleymani, J. Lichtenauer, T. Pun, and M. Pantic, "A multimodal database for affect recognition and implicit tagging," *IEEE Trans. Affect. Comput.*, vol. 3, no. 1, pp. 42–55, Jan.–Mar. 2012.
- [112] Y. Cimtay and E. Ekmekcioglu, "Investigating the use of pretrained convolutional neural network on cross-subject and cross-dataset EEG emotion recognition," *Sensors*, vol. 20, no. 7, p. 2034, 2020.
- [113] W.-L. Zheng *et al.*, "Vigilance estimation using a wearable EOG device in real driving environment," *IEEE Trans. Intell. Transp. Syst.*, vol. 21, no. 1, pp. 170–184, Jan. 2020.
- [114] D. Wu, C.-H. Chuang, and C.-T. Lin, "Online driver's drowsiness estimation using domain adaptation with model fusion," in *Proc. Int. Conf. Affect. Comput. Intell. Interact.*, Xi'an, China, Sep. 2015, pp. 904–910.
- [115] C.-S. Wei, Y.-P. Lin, Y.-T. Wang, C.-T. Lin, and T.-P. Jung, "A subject-transfer framework for obviating inter-and intra-subject variability in EEG-based drowsiness detection," *Neuroimage*, vol. 174, pp. 407–419, Jul. 2018.
- [116] L.-L. Chen, A. Zhang, and X.-G. Lou, "Cross-subject driver status detection from physiological signals based on hybrid feature selection and transfer learning," *Expert Syst. Appl.*, vol. 137, pp. 266–280, Apr. 2020.
- [117] H. Peng, F. Long, and C. Ding, "Feature selection based on mutual information criteria of max-dependency, max-relevance, and min-redundancy," *IEEE Trans. Pattern Anal. Mach. Intell.*, vol. 27, no. 8, pp. 1226–1238, Aug. 2005.
- [118] Y. Ming *et al.*, "EEG data analysis with stacked differentiable neural computers," *Neural Comput. Appl.*, vol. 32, pp. 7611–7621, Nov. 2018.
- [119] C. Szegedy *et al.*, "Intriguing properties of neural networks," in *Proc. Int. Conf. Learn. Represent.*, Apr. 2014, pp. 1–9.
- [120] P. Aricò, G. Borghini, G. Di Flumeri, N. Sciaraffa, and F. Babiloni, "Passive BCI beyond the lab: Current trends and future directions," *Physiol. Meas.*, vol. 39, no. 8, 2018, Art. no. 08TR02.



Dongrui Wu (Senior Member, IEEE) received the B.E. degree in automatic control from the University of Science and Technology of China, Hefei, China, in 2003, the M.E. degree in electrical engineering from the National University of Singapore, Singapore, in 2005, and the Ph.D. degree in electrical engineering from the University of Southern California, Los Angeles, CA, USA, in 2009.

He is currently a Professor with the School of Artificial Intelligence and Automation, Huazhong University of Science and Technology, Wuhan, China, where he is the Deputy Director of the Key Laboratory of Image Processing and Intelligent Control, Ministry of Education. He has more than 150 publications, including a book titled *Perceptual Computing* (Wiley/IEEE Press, 2010) and over 50 IEEE TRANSACTIONS papers. His research interests include affective computing, brain-computer interface, computational intelligence, and machine learning.

Prof. Wu received the IEEE Computational Intelligence Society Outstanding Ph.D. Dissertation Award in 2012, the IEEE TRANSACTIONS ON FUZZY SYSTEMS Outstanding Paper Award in 2014, the NAFIPS Early Career Award in 2014, the IEEE Systems, Man and Cybernetics Society Early Career Award in 2017, and the IEEE SMC Society Best Associate Editor Award in 2018. He was also a finalist of the USERN Prize in Formal Sciences in 2019 and another three best paper awards. His team won the First Prize in China BCI Competition in 2019. He was an Associate Editor of the IEEE TRANSACTIONS ON FUZZY SYSTEMS from 2011 to 2018, and has been an Associate Editor of the IEEE TRANSACTIONS ON FUZZY SYSTEMS since 2020, the IEEE TRANSACTIONS ON HUMAN-MACHINE SYSTEMS since 2014, the *IEEE Computational Intelligence Magazine* since 2017, and the IEEE TRANSACTIONS ON NEURAL SYSTEMS AND REHABILITATION ENGINEERING since 2019.



Yifan Xu (Graduate Student Member, IEEE) received the B.E. degree in automation from the Huazhong University of Science and Technology, Wuhan, China, in 2018, where she is currently pursuing the M.E. degree in control science and engineering with the School of Artificial Intelligence and Automation.

Her research interests include brain-computer interfaces and machine learning.



Bao-Liang Lu (Senior Member, IEEE) received the B.S. degree in instrument and control engineering from the Qingdao University of Science and Technology, Qingdao, China, in 1982, the M.S. degree in computer science and technology from Northwestern Polytechnical University, Xi'an, China, in 1989, and the Dr.Eng. degree in electrical engineering from Kyoto University, Kyoto, Japan, in 1994.

He was with the Qingdao University of Science and Technology from 1982 to 1986. From 1994 to 1999, he was a Frontier Researcher with the Bio-Mimetic Control Research Center, Institute of Physical and Chemical Research (RIKEN), Nagoya, Japan, and a Research Scientist with the RIKEN Brain Science Institute, Wako, Japan, from 1999 to 2002. Since 2002, he has been a Full Professor with the Department of Computer Science and Engineering, Shanghai Jiao Tong University, Shanghai, China. His current research interests include brain-like computing, neural networks, machine learning, brain-computer interface, and affective computing.

Prof. Lu received the IEEE TRANSACTIONS ON AUTONOMOUS MENTALDEVELOPMENT Outstanding Paper Award from the IEEE Computational Intelligence Society in 2018. He was the President of the Asia-Pacific Neural Network Assembly and the General Chair of the 18th International Conference on Neural Information Processing in 2011. He is currently an Associate Editor of the IEEE TRANSACTIONS ON COGNITIVE AND DEVELOPMENT SYSTEMS. He is currently a board member of Asia-Pacific Neural Network Society.